# An Autocatalytic Step in the Reaction Cycle of Hydrogenase from *Thiocapsa roseopersicina* Can Explain the Special Characteristics of the Enzyme Reaction

Judit Ősz and Csaba Bagyinka
Institute of Biophysics, Biological Research Center of the Hungarian Academy of Sciences, H-6701, Szeged, Hungary

ABSTRACT A moving front has been observed as a special pattern during the hydrogenase-catalyzed reaction of hydrogen uptake with benzyl viologen as electron acceptor in a thin-layer reaction chamber. Such fronts start spontaneously and at random times at different points of the reaction chamber; blue spheres are seen expanding at constant speed and amplitude. The number of observable starting points depends on the hydrogenase concentration. Fronts can be initiated by injecting either a small amount of completed reaction mixture or activated hydrogenase, but not by injecting a low concentration of reduced benzyl viologen. These characteristics are consistent with an autocatalytic reaction step in the enzyme reaction. The special characteristics of the hydrogen-uptake reaction in the bulk reaction (a long lag phase, and the enzyme concentration dependence of the lag phase) support the autocatalytic nature. We conclude that there is at least one autocatalytic reaction step in the hydrogenase-catalyzed reaction. The two possible autocatalytic schemes for hydrogenase are prion-type autocatalysis, in which two enzyme forms interact, and product-activation autocatalysis, where a reduced electron acceptor and an inactive enzyme form interact. The experimental results strongly support the occurrence of prion-type autocatalysis.

## INTRODUCTION

### Hydrogenases

Hydrogenases are metalloenzymes that catalyze the reaction $H_2 \rightleftharpoons 2\,H^+ + 2\,e^-$. Two distinct groups of hydrogenases can be defined, depending on the metal content of the protein. There are iron-only and [Ni-Fe] hydrogenases. The [Ni-Fe] enzymes are usually heterodimers involving a small (~30 kDa) and a large (~60 kDa) subunit, giving an overall molecular mass of ~90–100 kDa. The metals are organized into 2–3 FeS clusters and a Ni-Fe binuclear center. The Ni-Fe binuclear center or its ligand environment is believed to be the hydrogen-binding site because hydride/proton has been found close to the paramagnetic center (1–3), though the exact binding location of the hydrogen molecule has not yet been determined. The FeS clusters transfer the electrons from the Ni-Fe binuclear center to the terminal electron acceptor (4,5).

Though the enzymatic activity of hydrogenase is determined routinely, a number of contradictory results have been published. Despite the many features described in the hydrogenase reaction, the activity of this class of enzymes has not yet been thoroughly explained (6–10). It is known that hydrogenase needs activation to attain full activity (10,11). The characteristics and the members of the enzyme cycle are still a matter of dispute. Two hydrogenase catalysis models can be derived from the published data. Both models involve a double activation chain. Two inactive enzyme forms (Form A and Form B) of hydrogenase can be activated through several intermediates. Three hydrogenase forms take part in the enzyme cycle. In the triangular model, the enzyme cycle involves all three hydrogenase forms (Form S, Form C, and Form R (12–14)), whereas two enzyme cycles participate in the other model (15), each cycle involving two enzyme forms (the Form S/Form C and Form C/Form R cycles), Form C being common in the two cycles.

The kinetic characteristics of the hydrogen-uptake reaction of hydrogenase, obtained by conventional activity measurements, led us to propose an autocatalytic reaction step in the hydrogenase cycle or during the activation process (16). The autocatalytic behavior of an enzyme reaction may result in oscillating concentrations of enzyme intermediates and/or products contributing to the autocatalytic step. This behavior has already been investigated in the early phase of the hydrogenase-methyl viologen reaction (17). The results were evaluated on the assumption of an autocatalytic reaction in the hydrogenase kinetic cycle. The kinetic constants of the autocatalytic reaction were determined, and limits of the kinetic constants relating to the intramolecular (intraenzyme) reactions were set.

We now report new experimental evidence regarding the autocatalytic behavior of hydrogenase catalysis. Autocatalysis can explain several previously unexplained or misinterpreted findings concerning the activity of hydrogenases. Hydrogenase catalysis can also serve as an experimental example or model of a number of autocatalytic biological reactions (prion, autophosphorylation, etc.).

## MATERIALS AND METHODS

### Purification of hydrogenase

The stable [Ni-Fe] hydrogenase from *Thiocapsa roseopersicina* (HynSL) (18–20) was purified as described previously (17). Both partially (before

*Submitted January 8, 2005, and accepted for publication May 31, 2005.*

Address reprint requests to Csaba Bagyinka, Temesvári krt. 62, Szeged, PO Box 521, H-6701, Hungary. Tel.: 36-62-599605; Fax: 36-62-433133; E-mail: csaba@nucleus.szbk.u-szeged.hu.



0006-3495/05/09/1984/06 $2.00

doi: 10.1529/biophysj.105.059220

preparative gel electrophoresis) and fully purified enzymes were used for activity measurements, with no apparent difference in the results.

## Hydrogenase activity measurements

Hydrogenase activity can be measured by following the concentration of any of the substrates and/or products in the catalytic cycle. For this work, we utilized only hydrogen-uptake reactions and followed the appearance of the reduced electron acceptor (benzyl viologen from Sigma, St. Louis, MO).

The spatial distribution of the hydrogenase-catalyzed hydrogen-uptake reaction was followed both in a quartz cell and in a crystallization dish located in a small plexiglass anaerobic box. The atmosphere was changed and oxygen was removed by repeated evacuation and flushing with nitrogen gas. The reaction was initiated by changing the nitrogen atmosphere to hydrogen. The reaction mixture contained benzyl viologen (final concentration 100–400 $\mu$M) and hydrogenase in 20 mM phosphate buffer (pH 7).

The cells were stored on the desktop and photographs were taken at arbitrary time intervals.

In the plexiglass anaerobic chamber, 800 $\mu$l of the reaction mixture formed a 0.1-mm thin layer on the bottom of a crystallization dish. Due to the uneven surface, the curvature of the petri dish, and the side effects near the wall, the thickness of the solution varied slightly, depending on the position in the petri dish. This resulted in a somewhat uneven radial distribution of the spheres. The reaction was followed by video recording of the dish. The video was then assembled and maintained by the computer program Adobe Premier 5.1 or a freeware program, avi2mpg1 1.10.

Seeding was performed by injecting a small amount (1–3 $\mu$l) of seeding material (completed reaction mixture, activated hydrogenase, inactive hydrogenase, reduced benzyl viologen, or oxidized benzyl viologen) with a Hamilton syringe into the reaction chamber through a rubber stopper, while the reaction chamber was flushed with hydrogen.

Conventional uptake measurements were performed in an anaerobic quartz cell sealed with a Suba Seal rubber stopper. The reaction mixture contained benzyl viologen (final concentration 400 $\mu$M) and hydrogenase in 20 mM phosphate buffer (pH 7). The atmosphere was changed by flushing the cell with nitrogen and then with hydrogen gas, for 10 min each. The absorption change at 600 nm at 40°C was followed by means of a Unicam ultraviolet/visible UV2 spectrophotometer (Unicam, Cambridge, UK) and the Vision 3.41 program.

To activate the hydrogenase, it was incubated in sealed glass vessels at room temperature for 2 days. After the change of the atmosphere to nitrogen and subsequently to hydrogen, the vessels were transferred into an anaerobic chamber (Bactron IV, Cornelius, OR) so as to avoid oxygen leakage into the vessels. The atmosphere in the chamber was 5% hydrogen + 95% nitrogen. After 2 days of incubation, samples were placed into normal cells and conventional uptake activities were measured.

# RESULTS AND DISCUSSION

## Spatial distribution of hydrogenase-uptake reaction

A special pattern of hydrogenase catalysis kinetics was observed both in the anaerobic cell and in the anaerobic thin-layer reaction mixture (Fig. 1). In the reactions in the cell, the reaction starts at a specific point, from where it spreads throughout the cell. The reaction can start in the bulk of the solution (Fig. 1 *A*, *bottom*) or at the surface (Fig. 1 *A*, *top*). Accordingly, it is concluded that the starting point has nothing to do with the liquid-gas interface or with uneven diffusion of the hydrogen gas into the reaction mixture. This behavior was earlier observed for the *D. gigas* hydrogenase-catalyzed hydrogen-uptake reaction (10), but no conclusion was drawn from this fact.

The autocatalytic wavefront can be seen much more easily by using a thin-layer reaction chamber. In the thin-layer reactions (Fig. 1 *B*), numerous starting points develop in time. The fronts start spontaneously and at random times at different points in the reaction chamber; blue spheres of reduced benzyl viologen are seen expanding at constant speed and amplitude (Fig. 2, *A* and *B*). The number of starting points in the reaction chamber depends on the hydrogenase concentration. The higher the concentration, the more spheres start to grow. The spheres collide, interfere, and overlap, and at the end of the reaction the whole of the initially completely colorless reaction mixture is blue.

The front can be initiated by injecting a small amount of either a completed reaction mixture or activated hydrogenase. This means that a product(s) of the reaction accelerates the reaction, acting as a catalyst. However, the reaction cannot be initiated by injecting anaerobic buffer, a low concentration of reduced benzyl viologen or nonactivated (but anaerobic) hydrogenase.

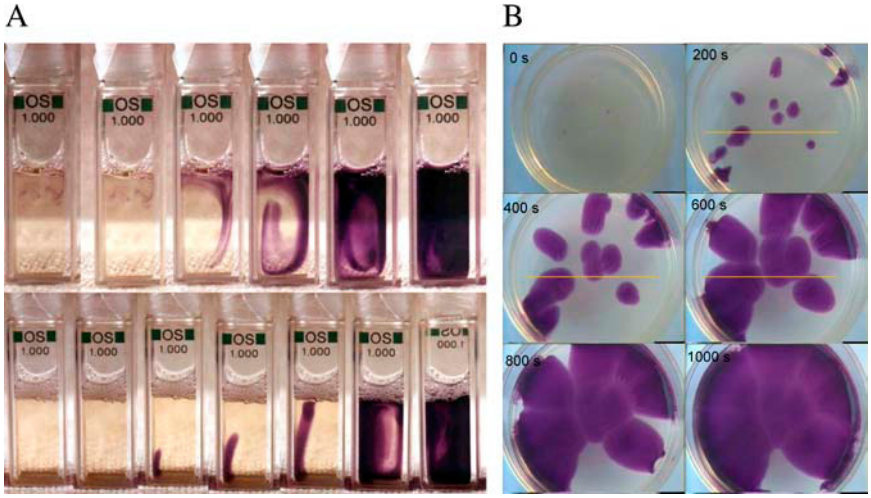


FIGURE 1 Spatial distribution of hydrogenase-catalyzed hydrogen-uptake reaction. (*A*) Uptake reaction in cells. Photos on two sets of activity measurements taken at arbitrary intervals. (*B*) Thin-layer spatial distribution of hydrogenase-catalyzed hydrogen-uptake activity. The yellow line represents the line of calculations for Fig. 2. (The full reaction movie is available as Supplementary Material in mpeg format.)

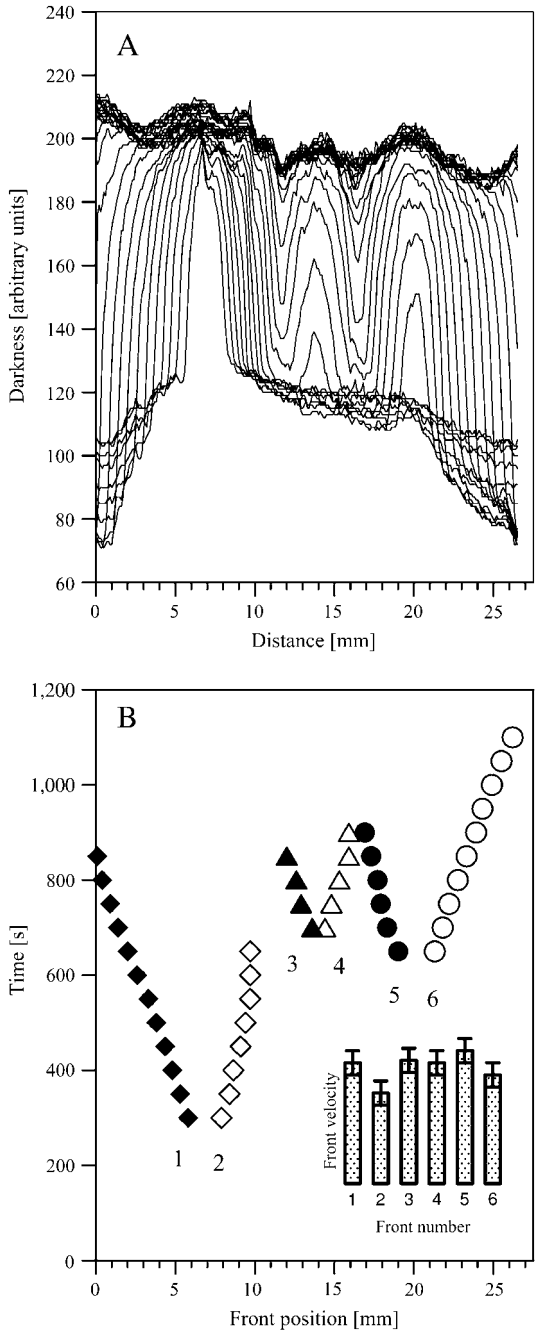


FIGURE 2 Profile of the wavefronts at different times and time-space plot of a thin-layer reaction of hydrogenase-catalyzed hydrogen uptake. (*A*) The darkness of individual pixels (which is proportional to the reduced benzyl viologen concentration) of time frames along the yellow line in Fig. 1 has been calculated and plotted. There were three different starting points at different times, the reaction of which crossed the line of calculation. Accordingly, three fronts developed in time at ~7, 14, and 20 mm from the left end of the line of calculations (see also Fig. 1). The spots also slowly increase in the vertical dimension. The darkness is not at its maximum from the very beginning of the appearance of the spot, indicating that the layer thickness does not interfere with the reaction. The darkness values level off at their maximum value at the end of the reaction, and the whole reaction chamber becomes blue. (*B*) Front positions at different times. The values were calculated from the time-versus-space plot in panel *A*, using the maximum values of the first derivative of the time-versus-space plot. The front position-versus-time curve is linear for every front; deviation from linearity occurs only when two fronts collide. The slopes of the front position-versus-time curve vary slightly due to the uneven layer thickness in the petri dish and because the line of calculation does not cross the midpoint of every spot. (*Insert*) Initial front velocities calculated from the first few points of the front position-versus-time curve. For an ideal thin-layer autocatalytic reaction and if the front positions are calculated from the midpoint of the reaction spot, the velocities should be equal.

A reaction type that can produce fronts of soluble reactants moving at constant speed and amplitude, and that can be seeded by reaction products, is a nonlinear reaction (21–26). Such characteristics are typical signs of an autocatalytic step in the hydrogenase-catalyzed reaction. The only question that arises, therefore, is the nature of the autocatalytic partners in the autocatalytic reaction. The two possibilities for interacting partners are any two enzyme forms, or an enzyme form and a product of the reaction (in our case reduced benzyl viologen or the proton). Because protons are common and are present in high concentration in any buffer solution, and because the long incubation of hydrogenase under a nitrogen atmosphere did not alter the reaction pattern, we can rule out the proton as an interacting autocatalytic partner.

When the thin-layer reaction mixture was exposed to an excimer laser, which led to a partial reduction of oxidized benzyl viologen at the laser spot in the solution (17,27), no new starting point developed at the point of the laser flash, even if the diameter of the laser flash was varied in the millimeter range, which is much more than the thickness of the reaction layer. In this case, too, the spontaneous and random starting points appeared later, though at different points of the reaction chamber. This confirms the fact that low-concentration seeding with a product (reduced benzyl viologen) does not initiate a starting point in the thin-layer hydrogenase-catalyzed hydrogen-uptake reaction, which is an indication that reduced benzyl viologen (a product) is not an autocatalytic partner in the autocatalytic reaction. Seeding with activated hydrogenase at a much lower (one-tenth) concentration than that in the reaction chamber, however, resulted in the immediate seeding of a starting point in the reaction mixture.

To summarize the thin-layer reaction results, we can conclude that, according to the International Union of Pure and Applied Chemistry Compendium of Chemical Terminology (http://www.iupac.org/publications/compendium/) definition of an autocatalytic reaction, the hydrogenase cycle, or the hydrogenase activation phase includes an autocatalytic step. Because no other possibilities appear to remain, this autocatalytic step almost certainly occurs between two different enzyme forms. It should be noted that, in order for the autocatalytic reaction to start, not merely anaerobic conditions, but also a hydrogen atmosphere must be maintained. Storage of the hydrogenase under a nitrogen atmosphere and change of the atmosphere to hydrogen after a considerable time did not alter the pattern of behavior of the

reaction. This means that hydrogen is also necessary for the autocatalytic reaction, which suggests that one of the two interacting enzyme forms is located after the hydrogen-binding reaction in the enzyme cycle. It is still an open question as to whether the other enzyme form also participates in the enzyme cycle, or in the phase of the hydrogenase activation.

## The lag phase of the hydrogenase reaction

Hydrogenase-catalyzed hydrogen uptake almost always starts with a considerable lag period (6–8,13,28,29). Typical hydrogen-uptake reaction curves for hydrogenase are presented in Fig. 3. The main characteristics of the hydrogenase-uptake reaction are:

1. The lag period for hydrogenase catalysis can be several hours long, and in extreme cases several days. There is no observable reaction during this time. After the lag phase, the velocity of the reaction increases very rapidly (Fig. 3 *A*); the overall reaction curve is not exponential.

   A lag period can occur when there is a slow activation process ($k1$) in the catalytic cycle, followed by a faster enzyme reaction. In this case, the reaction velocity initially has a small value that depends on the activated portion, $p$, of the enzyme at $t = 0$, and the velocity increases exponentially until it attains a constant value (which is proportional to $k2$). The lag phase is defined as the length of time necessary for this constant velocity to be reached. This conventional lag phase is further characterized by its dependence on the kinetic constant of the activation process ($k1$) and on the distribution of the enzyme forms ($p$), but it does not depend on the overall enzyme concentration (the length of the lag period is $(1 - p)/k1$).

   The characteristics of the lag phase of the hydrogenase-uptake reaction observed here are completely different from this picture. We can conclude (as we will discuss later) that the observed lag phase is the sum of a conventional lag phase and an autocatalytic lag phase.
2. The total reaction time from the end of the lag period up to equilibrium is usually only several minutes, which is considerably shorter than the lag time of the reaction.

   There is a possibility that, during hydrogenase catalysis, the reduced electron acceptor (benzyl viologen) that is produced interacts with dissolved oxygen gas that was not removed sufficiently from the reaction mixture and the oxygen gas oxidizes the reduced electron acceptor, falsifying the results of the uptake experiment. If the overall reaction time after the lag period is compared with the length of the lag period itself, however, it is apparent that the amount of residual oxygen in the reaction mixture should be several orders of magnitude higher than the amount of the electron acceptor to explain the ratio of several hours (days) versus several minutes for the lag period and the full reaction up to equilibrium. Such a high oxygen concentration in these experiments is impossible. This confirms that there is no appreciable side reaction, i.e., the lag phase is an inherent property of the hydrogenase-uptake reaction itself.
3. The second derivative of the detected product concentration versus time curve has a maximum at the end of the lag period (Fig. 3 *A*, *trace delta*).

   This behavior is also characteristic of an autocatalytic reaction and cannot be found in a simple enzyme reaction cycle (30). We have used this maximum in the second derivative to determine the length of the lag phase.
4. The length of the lag period depends on the enzyme concentration (Fig. 3 *B*).

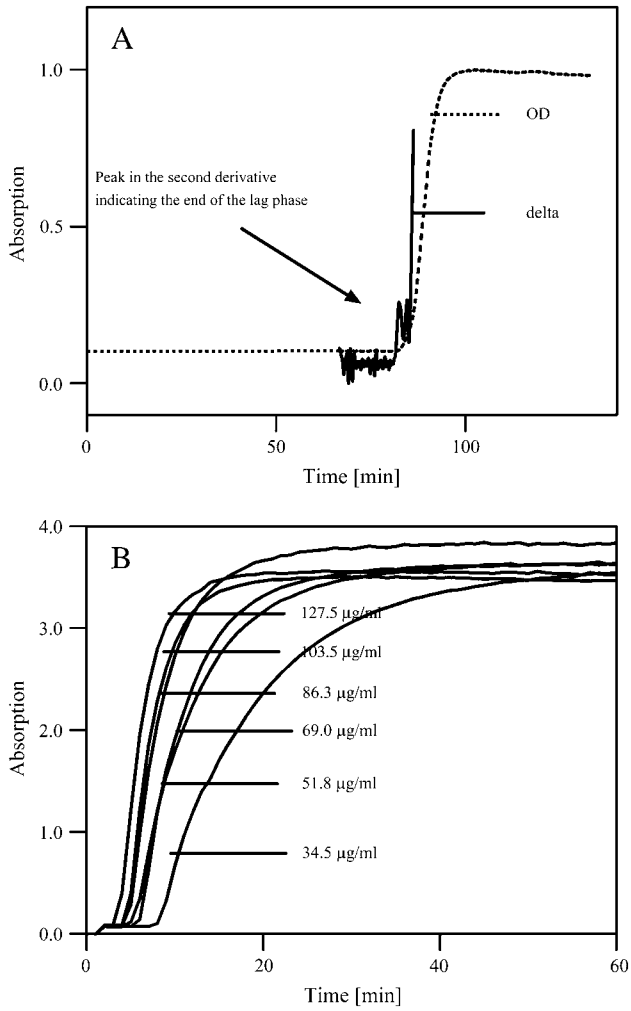


FIGURE 3 Experimental hydrogenase-catalyzed hydrogen-uptake kinetics. (*A*) A typical kinetic curve displaying a long lag period of hydrogenase uptake (*OD*) and the second derivative of the measured kinetics at around the end of the lag phase (*delta*). In this experiment, only 100 $\mu$M benzyl viologen was used. (*B*) Hydrogenase uptake experiments at different enzyme concentrations. The enzyme was incubated under hydrogen for 2 days, so the lag period lengths are much shorter than in panel *A*.

The lag phase is the sum of the autocatalytic and conventional lag phases. Unlike conventional lag phases, the

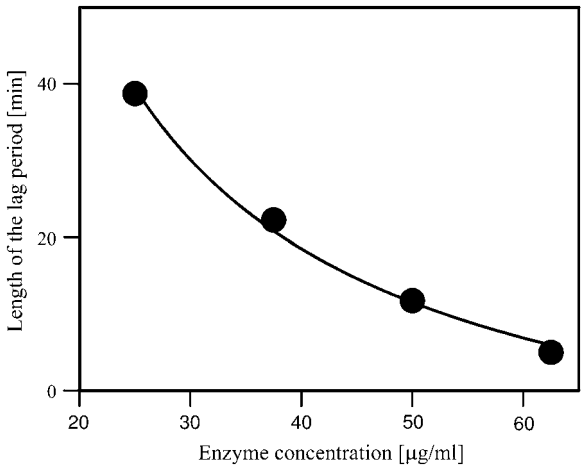


FIGURE 4 The lag phase versus enzyme concentration dependence. The length of the lag phase varies with the enzyme concentration according to a hyperbolic function. The dependence follows the function $y = B + A/x$. (●) Experimental data; (*solid line*) fitted curve.

length of the hydrogenase catalysis lag period depends on the enzyme concentration. For hydrogenase catalysis, the lag phase exhibits a hyperbolic dependence on the enzyme concentration (Fig. 4). The higher the concentration, the shorter the lag period. If the lag phase is decreased, by increase of the enzyme concentration, a point can be reached where the autocatalytic reaction step becomes negligible and there is no observable autocatalytic lag phase at all. At this high enzyme concentration, the reaction behaves as a non-autocatalytic reaction.

This situation is very similar to that of the well-known Landolt autocatalytic reaction (31), which is commonly used to determine catalyst concentrations (usually those of metal ions) in inorganic analytical chemistry. Similarly, the enzyme concentration versus lag phase dependence can be used to calibrate the enzyme concentration if the conventional lag phase can be diminished. This is usually achieved by activating the enzyme fully (10). The lag phase persists for this fully activated enzyme, as demonstrated in Fig. 3 *B*, but its observation is more difficult because the concentration of the active enzyme form is increasing and the lag period is considerably shortened. Careful examination of the reaction, however, reveals that, if the activated enzyme in a condition where no lag period is observed is diluted, the lag period will reappear.

To summarize the results, we have found experimental evidence of an autocatalytic reaction step in the reaction of hydrogenase-catalyzed hydrogen uptake. The autocatalytic step most probably involves an interaction between two hydrogenase forms.

## SUPPLEMENTARY MATERIAL

An online supplement to this article can be found by visiting BJ Online at http://www.biophysj.org.

The authors are grateful to L. Tiszai and P. Galajda for their kind help in shrinking and maintaining the video records, and to Gy. Váró for help in the excimer laser experiments.

This work was supported by the Hungarian Science Foundation (OTKA T 029008, OTKA T 049276, and OTKA-NSF 35540).

## REFERENCES

1. Whitehead, J. P., R. J. Gurbiel, C. Bagyinka, B. M. Hoffman, and M. J. Maroney. 1993. The hydrogen binding site in hydrogenase: 35 GHz ENDOR and XAS studies of the Ni-C active form and the Ni-L photoproduct. *J. Am. Chem. Soc.* 115:5629–5635.
2. Brecht, M., M. van Gastel, T. Buhrke, B. Friedrich, and W. Lubitz. 2003. Direct detection of a hydrogen ligand in the [NiFe] center of the regulatory $H_2$-sensing hydrogenase from *Ralstonia eutropha* in its reduced state by HYSCORE and ENDOR spectroscopy. *J. Am. Chem. Soc.* 125:13075–13083.
3. Foerster, S., M. Stein, M. Brecht, H. Ogata, Y. Higuchi, and W. Lubitz. 2003. Single-crystal EPR studies of the reduced active site of [NiFe] hydrogenase from *Desulfovibrio vulgaris* Miyazaki F. *J. Am. Chem. Soc.* 125:83–93.
4. Sherman, M. B., E. V. Orlova, E. A. Smirnova, S. Hovmoller, and N. A. Zorin. 1991. Three-dimensional structure of the nickel-containing hydrogenase from *Thiocapsa roseopersicina*. *J. Bacteriol.* 173:2576–2580.
5. Volbeda, A., M. H. Charon, C. Piras, E. C. Hatchikian, M. Frey, and J. C. Fontecilla-Camps. 1995. Crystal-structure of the nickel-iron hydrogenase from *Desulfovibrio gigas*. *Nature.* 373:580–587.
6. Fisher, H. F., A. I. Krasna, and D. Rittenberg. 1954. The interaction of hydrogenase with oxygen. *J. Biol. Chem.* 209:569–578.
7. Krasna, A. I., and D. Rittenberg. 1954. The mechanism of action of the enzyme hydrogenase. *J. Am. Chem. Soc.* 76:3015–3020.
8. Anand, S. R., and A. I. Krasna. 1965. Catalysis of the $H_2$-HTO exchange by hydrogenase. A new assay for hydrogenase. *Biochemistry.* 4:2747–2753.
9. Yagi, T., M. Tsuda, and H. Inokuchi. 1973. Kinetic studies on hydrogenase. Parahydrogen-orthohydrogen conversion and hydrogen-deuterium exchange reactions. *J. Biochem.* (*Tokyo*). 73:1069–1081.
10. Fernandez, V. M., E. C. Hatchikian, and R. Cammack. 1985. Properties and reactivation of two different deactivated forms of *Desulfovibrio gigas* hydrogenase. *Biochim. Biophys. Acta.* 832:69–79.
11. Lissolo, T., S. Pulvin, and D. Thomas. 1985. Reactivation of the hydrogenase from *Desulfovibrio gigas* by hydrogen. Influence of redox potential. *J. Biol. Chem.* 259:11725–11729.
12. De Lacey, A. L., J. Moiroux, and C. Bourdillon. 2000. Simple formal kinetics for the reversible uptake of molecular hydrogen by [Ni-Fe] hydrogenase from *Desulfovibrio gigas*. *Eur. J. Biochem.* 267:6560–6570.
13. Vignais, P. M., L. Cournac, E. C. Hatchikian, S. Elsen, L. T. Serebryakova, N. A. Zorin, and B. Dimon. 2002. Continuous monitoring of the activation and activity of [NiFe]-hydrogenases by membrane-inlet mass spectrometry. *Int. J. Hydrogen Energy.* 27:1441–1448.
14. Armstrong, F. A. 2004. Hydrogenases: active site puzzles and progress. *Curr. Opin. Chem. Biol.* 8:133–140.
15. Kurkin, S., S. J. George, R. N. F. Thorneley, and S. P. J. Albracht. 2004. Hydrogen-induced activation of the [NiFe]-hydrogenase from *Allochromatium vinosum* as studied by stopped-flow infrared spectroscopy. *Biochemistry.* 43:6820–6831.
16. Ősz, J., and C. Bagyinka. 2001. Experimental evidences for autocatalytic reaction cycle of hydrogenase enzyme. *Eur. J. Biochem.* 268:250.
17. Bagyinka, C., J. Ősz, and S. Száraz. 2003. Autocatalytic oscillations in the early phase of the photoreduced methyl viologen-initiated fast kinetic reaction of hydrogenase. *J. Biol. Chem.* 278:20624–20627.

18. Bagyinka, C., K. L. Kovacs, and E. Rak. 1982. Localization of hydrogenase in *Thiocapsa roseopersicina* photosynthetic membrane. *Biochem. J.* 202:255–258.

19. Cammack, R., C. Bagyinka, and K. L. Kovacs. 1989. Spectroscopic characterization of the nickel and iron-sulphur clusters of hydrogenase from the purple photosynthetic bacterium *Thiocapsa roseopersicina*. 1. Electron spin resonance spectroscopy. *Eur. J. Biochem.* 182: 357–362.

20. Rakhely, G., A. Colbeau, J. Garin, P. M. Vignais, and K. L. Kovacs. 1998. Unusual organization of the genes coding for HydSL, the stable [NiFe]hydrogenase in the photosynthetic bacterium *Thiocapsa roseopersicina* BBS. *J. Bacteriol.* 180:1460–1465.

21. Showalter, K. 1981. Trigger waves in the acidic bromate oxidation of ferroin. *J. Phys. Chem.* 85:440–447.

22. Weitz, D. M., and I. R. Epstein. 1984. Spatial waves in the reaction of chlorite with iodide. *J. Phys. Chem.* 88:5300–5304.

23. Bazsa, G., and I. R. Epstein. 1985. Traveling waves in the nitric acid-iron(II) reaction. *J. Phys. Chem.* 89:3050–3053.

24. Harrison, J., and K. Showalter. 1986. Propagating acidity fronts in the iodate-arsenous acid reaction. *J. Am. Chem. Soc.* 90:225–226.

25. Needham, D. J., and J. H. Merkin. 1992. The effect of geometrical spreading in two and three dimensions on the formation of travelling wavefronts in a simple, isothermal, chemical system. *Nonlinearity.* 5:413–452.

26. Epstein, E. R., and J. A. Pojman. 1998. An Introduction to Nonlinear Chemical Dynamics. Oscillations, Waves, Patterns, and Chaos. Oxford University Press, New York, NY; Oxford, UK.

27. Czege, J., C. Bagyinka, and K. L. Kovács. 1989. Transient kinetics of flavocytochrome c photoreduction by methyl viologen. *Photochem. Photobiol.* 50:697–700.

28. Berlier, Y. M., G. Fauque, P. A. Lespinat, and J. LeGall. 1982. Activation, reduction and proton-deuterium exchange reaction of the periplasmic hydrogenase from *Desulfovibrio gigas* in relation with the role of cytochrome $c_3$. *FEBS Lett.* 140:185–188.

29. Higuchi, Y., H. Ogata, K. Miki, N. Yasuoka, and T. Yagi. 1999. Removal of the bridging ligand atom at the Ni-Fe active site of [NiFe] hydrogenase upon reduction with $H_2$, as revealed by X-ray structure analysis at 1.4 A resolution. *Struct. Fold. Des.* 7:549–555.

30. Ősz, J., G. Bodó, R. M. M. Branca, and C. Bagyinka. 2005. Theoretical calculations on hydrogenase kinetics: explanation of the lag phase and the enzyme concentration dependence of the activity of hydrogenase-catalyzed hydrogen-uptake. *Biophys. J.* 89:1957–1964.

31. Ibison, P. 1992. Reduction and analysis of oscillatory Landolt mechanisms. *J. Phys. Chem.* 96:6321–6325.